Thermodynamic Characteristics of Tropical Cyclones with Rapid Intensity Change over the Coastal Waters of China*

YU Yubin† (于玉斌) and YAO Xiuping (姚秀萍)

China Meteorological Administration Training Center, Beijing 100081

(Received October 12, 2010)

ABSTRACT

In order to investigate the different thermodynamic mechanisms between rapid intensifying (RI) and rapid weakening (RW) tropical cyclones (TCs), the thermodynamic structures of two sets of composite TCs are analyzed based on the complete-form vertical vorticity tendency equation and the NCEP/NCAR reanalysis data. Each composite is composed of five TCs, whose intensities change rapidly over the coastal waters of China. The results show that the maximum apparent heating source Q_1 exists in both the upper and lower troposphere near the RI TC center, and Q_1 gets stronger at the lower level during the TC intensification period. But for the RW TC, the maximum Q_1 exists at the middle level near the TC center, and Q_1 gets weaker while the TC weakens. The maximum apparent moisture sink Q_2 lies in the mid troposphere. Q_2 becomes stronger and its peak-value height rises while TC intensifies, and vice versa. The increase of diabatic heating with height near the TC center in the mid-upper troposphere and the increase of vertical inhomogeneous heating near the TC center in the lower troposphere are both favorable to the TCs' rapid intensification; otherwise, the intensity of the TC decreases rapidly.

Key words: coastal waters, tropical cyclone, rapid intensity change, thermodynamic mechanism

Citation: Yu Yubin and Yao Xiuping, 2011: Thermodynamic characteristics of tropical cyclones with rapid intensity change over the coastal waters of China. *Acta Meteor. Sinica*, **25**(4), 467–477, doi: 10.1007/s13351-011-0407-y.

1. Introduction

The diabatic heating, especially the latent heating, oceanic sensible heat flux, and radiative cooling, is the main source of energy for the development and maintenance of tropical cyclones (TCs) (Anthes, 1982). In most cases, the change of TC intensity depends on three factors: initial intensity of the TC, thermal dynamic state of the atmosphere, and the air-sea heat exchange in the upper layer of the ocean under the TC core (Emanuel, 1999). TC intensity is significantly enhanced by strong heating. If the maximum heating is shifted from 300 to 200 hPa, the anticyclone divergence strengthens at 200 hPa and the TC deepens at 500 hPa (Chen et al., 2002). The rapid intensifying (RI) TCs over coastal waters are always difficult to forecast and usually cause serious disasters. Liang et al. (2003) performed a diagnostic analysis on the TC Vongfong (2002), which intensified over the coastal waters of China. Their results showed that the intensification of Vongfong (2002) was associated with the drier and colder air intrusion from the mid troposphere, which affected the TC's inner thermodynamic structure and strengthened its potential instability. Also, the vertical transport of latent heat in the boundary layer was conducive to the intensification of Vongfong (2002) (Yan et al., 2003). The latent heating warms the vortex, increases the potential energy of the vortex, maintains the TC warm core structure, and enhances the transformation from potential to kinetic energy within the vortex (Xu, 2007). Yang and Ding (1985) studied contributions of static stability parameters and heating to the genesis and development of TCs using the nonlinear theory. The TC development is influenced by both inertial stability and stratification stability (Liu and Ni, 1983). Under the nonlinear

*Supported by the National Natural Science Foundation of China (40875030, 40730948, and 40575018) and China Meteorogical Administration Climate Change Program (CCSF2007-13).
†Corresponding author: yuyb@cma.gov.cn.
(Chinese version published in Vol. 68, No. 1, 48–58, 2010)

stratification condition, change of the heating strength usually causes an abrupt change of the stratification state (Liu and Liu, 1984). The anomalous development of the TC is related not only to the convective heating and dissipation, but also to nonlinear advection of momentum and thermal flux through the lateral boundary and transfer of sensible and latent heat fluxes over the underlying surface (Xu, 1991). The diabatic heating is an important factor in the rapid intensity change of TCs (Xia et al., 1995; Zheng and Xia, 1996). With the application of new observational data, new methods have been developed to explore thermal characteristics of TCs, and many studies have investigated the thermodynamics of the TC eye in recent years (Schneider and Barnes, 2005; Halverson et al., 2006).

The release of latent heat by condensation is the main source of energy for TC development and it is mainly contributed by the cumulus convection. Generally, there are two methods to calculate the vertical transport of cumulus convection (Yanai et al., 1973). Firstly, it is regarded as a residue to the large-scale terms calculated by use of large-scale data. Secondly, it is directly calculated by the cloud-resolving model. Apparent heating source Q_1 and apparent moisture sink Q_2 calculated by large-scale variables (or grid-scale mean variables) can reflect the latent heat release of cumulus convection and vertical transport of heat and moisture. Typically, Q_1 and Q_2 are calculated following Yanai et al. (Yanai et al., 1973; Johnson, 1984; Ding, 1989). The apparent heating Q_1 of the large-scale motion system consists of the heating due to radiation, the release of latent heat by net condensation, and vertical convergence of the vertical eddy transport of sensible heat. The apparent moisture sink Q_2 is due to the net condensation and vertical divergence of the vertical eddy transport of moisture (Yanai et al., 1973).

Research on atmospheric dynamics has been dominant in the past several decades (Wu, 2002). Knowledge on atmospheric thermodynamics was promoted by the concept and theory of dissipative systems (Cao, 2005). A TC takes energy from the environment to survive and develop, which is undoubtedly a dissipative system in the non-equilibrium thermal state. The complete-form vorticity equation must be used in the studies relevant to external heating and dissipation (Wu and Liu, 2000). Due to limitations in technology and data, evolution of the thermal structure of a TC system in its rapid intensity change period has rarely been studied in the past (Emanuel, 1999).

Using composite datasets, thermal characteristics of TCs undergoing rapid intensity changes are analyzed in this paper. The role of diabatic heating in the rapid intensity change of a TC is diagnosed using the complete vertical vorticity equation, and the thermal characteristics of the TC with changing intensities over the coastal waters of China are revealed.

2. Data and methods

Yu et al. (2007) defined the standard of the TC rapid intensity change and analyzed the vertical structure of two sets of composite TCs, which intensified and weakened rapidly over the coastal waters of China. In this study, the NCEP FNL (Final) Operational Global Analysis 4-time daily data in 2000–2006 with a horizontal resolution of $1°\times1°$ and 11 vertical levels from 1000 to 100 hPa are used to investigate the thermodynamic features of two sets of composite TCs. Each set is composed of 5 TCs, whose intensity changes rapidly (i.e., rapid intensifying or rapid weakening (RW)) over the coastal waters of China. The composite area covers $40°\times40°$ latitude by longitude. The composite TC center is set at the coordinate origin, and the x and y axes represent zonal and meridional directions, respectively. The basic information of the TC cases is given in Table 1.

3. Variations of the apparent heating source Q_1 and apparent moisture sink Q_2

Q_1 and Q_2 are calculated by the scheme proposed by Yanai et al. (Yanai et al., 1973; Johnson, 1984; Ding, 1989) as follows:

$$Q_1 = \frac{\partial \overline{S}}{\partial t} + \overline{\nabla \cdot SV} + \frac{\partial \overline{S}\overline{\omega}}{\partial p} = Q_R + L(c-e) - \frac{\partial}{\partial p}\overline{S'\omega'}, \tag{1}$$

Table 1. Basic information of the TCs with rapid intensity variations

TC category	TC number	Time (BT)	Center	Central pressure (hPa)	Maximum wind speed (m s^{-1})	Pressure variation per 6 h (hPa)	Wind speed variation per 12 h (m s^{-1})
RI	0016	2000-09-07 T08	(18.9°N, 115.9°E)	980	30	–5	8
	0107	2001-07-24 T14	(20.6°N, 117.0°E)	980	30	–10	10
	0116	2001-09-20 T02	(22.6°N, 117.9°E)	985	20	–3	10
	0220	2002-09-25 T08	(17.7°N, 109.6°E)	998	18	–2	8
	0518	2005-09-25 T14	(19.0°N, 112.4°E)	940	50	–20	15
RW	0016	2000-09-09 T14	(18.2°N, 109.7°E)	975	33	15	–10
	0307	2003-07-24 T08	(21.1°N, 111.9°E)	950	45	25	–15
	0313	2003-09-02 T14	(22.3°N, 116.5°E)	960	40	15	–10
	0320	2003-11-19 T02	(19.7°N, 108.6°E)	990	23	20	–12
	0601	2006-05-17 T14	(21.3°N, 116.0°E)	960	40	10	–5

$$Q_2 = -L(\frac{\partial \overline{q}}{\partial t} + \overline{\nabla \cdot qV} + \frac{\partial \overline{q}\,\overline{\omega}}{\partial t})$$
$$= L(c-e) - L\frac{\partial}{\partial p}\overline{q'\omega'}. \quad (2)$$

Most of the notations in Eqs. (1) and (2) are conventional. $S = C_pT + gz$ is the dry static energy, L the latent heat by condensation, Q_{R} the heating rate due to radiation, c the rate of condensation per unit mass of air, and e the rate of re-evaporation of cloud droplets. The horizontal averages are denoted by $\overline{(\ )}$, and the deviations from the horizontal averages are denoted by $(\ )'$.

Equation (1) shows that Q_1 consists of the radiative heating, the release of latent heat by net condensation, and the vertical convergence of vertical eddy transport of sensible heat. Equation (2) is the moisture continuity equation expressed in units of heating rate, with Q_2 being a measure of the apparent moisture sink due to the net condensation and vertical divergence of vertical eddy transport of moisture. Q_1 denotes the variation of dry static energy. When air temperature rises resulting in upward motion, the dry static energy increases and Q_1 is positive, and vice versa. Q_2 denotes the latent heat release caused by possible changes of water vapor in the air. When the water vapor is reduced due to condensation or sublimation, the latent heat releases and Q_2 is positive, and vice versa. The distributions of Q_1 and Q_2 demonstrate the effect of cumulus convection on the vertical transport of heat and moisture.

From Eqs. (1) and (2), we obtain

$$Q_1 - Q_2 - Q_{\mathrm{R}} = -\frac{\partial}{\partial p}\overline{(S' + Lq')\omega'} = \frac{\partial}{\partial p}\overline{h'\omega'}, \quad (3)$$

where $\overline{h'\omega'}$ is a measure of the vertical eddy transport of total heat and may be used to measure the activity of cumulus convection.

The zonal vertical sections of Q_1 and Q_2 through the composite TC center are given in Fig. 1. There exist Q_1/Q_2 columns near the TC center from the low to high levels. Figure 1 shows that the maximum Q_1 exists at 200 and 800 hPa near the RI TC center (Fig. 1a), and Q_1 becomes increasingly larger when TC intensifies at 800 hPa (figure omitted). But for the RW TC, the maximum Q_1 appears at 500 hPa near the TC center (Fig. 1c), and Q_1 becomes increasingly smaller when the TC weakens (figure omitted). The maximum Q_2 is located in the mid troposphere (Figs. 1b, 1d), and Q_2 becomes increasingly larger when the TC intensifies, and vice versa (figure omitted).

Taking the composite TC center as the origin, Q_1 and Q_2 for RI and RW TCs are averaged over the region within a radius of 5 latitude degrees to the origin so as to analyze their vertical distributions and variations (Fig. 2).

For the RI TC, from 12 h before the RI time to 12 h after the RI time (Figs. 2b-d), the value of Q_1 is larger than that of Q_2, and Q_1 and Q_2 differ greatly in the mid-upper troposphere. Moreover, convection is more significant at mid-upper levels according to Eq. (3). But for the RW TC, the value of Q_2 is larger than Q_1 below 600 hPa in the lower troposphere, while it is

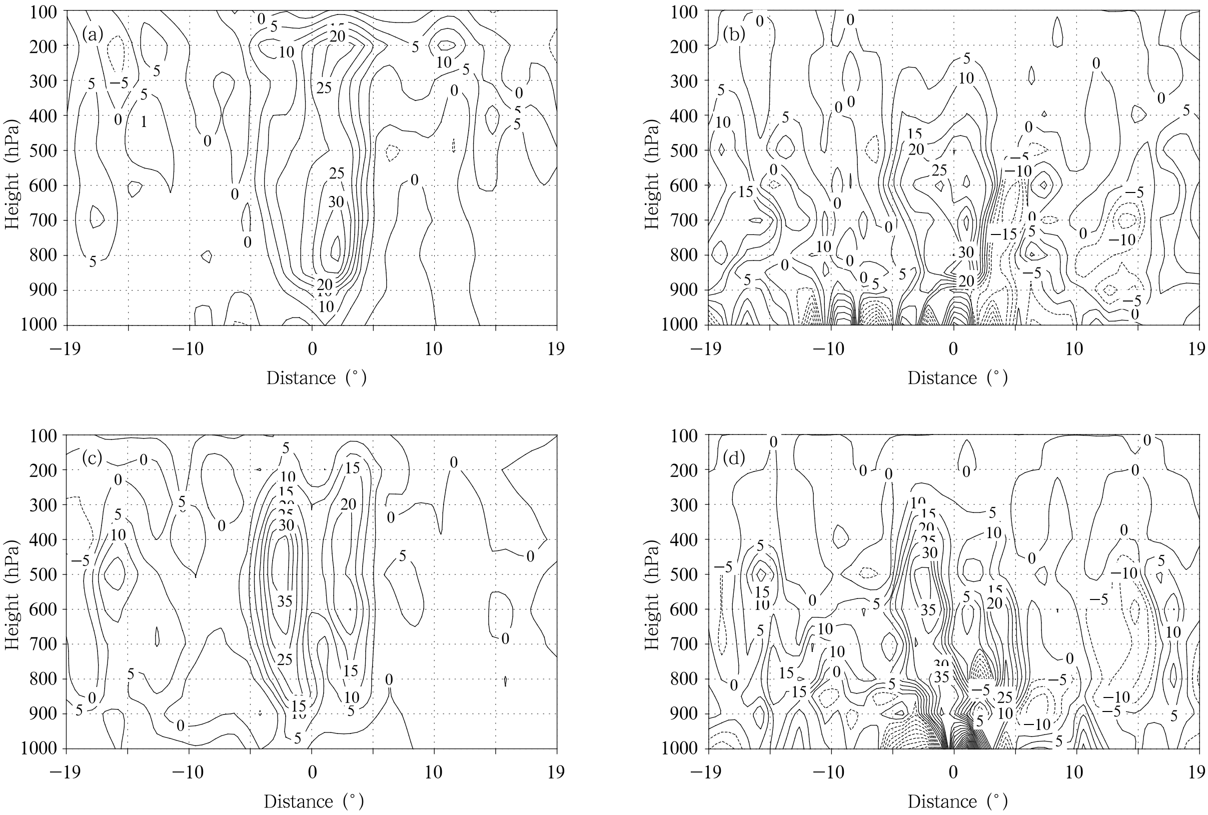

Fig. 1. Vertical cross-sections of apparent heating source Q_1 (10^{-5} K s^{-1}) and moisture sink Q_2 (10^{-5} K s^{-1}) through the composite TC center at the RI time (a, b) and the RW time (c, d), respectively.

opposite above 600 hPa in the mid-upper troposphere (Figs. 2e-h). Furthermore, the distributions of Q_1 and Q_2 are similar, which indicates that the convection is not significant.

The values of Q_1 and Q_2 and their peak-value heights alter during the rapid intensity change period of the TC. The values of Q_1 and Q_2 remain increasing during the RI process and decreasing during the RW process. During the TC rapid intensity change period, the peak-value height of Q_1 changes little, and it is roughly located in the upper troposphere during the RI process and in the mid troposphere during the RW process. The peak-value height of Q_2 rises continually during the RI process (Figs. 2a-c), at 850, 500, and 400 hPa 24 h before RI, 12 h before RI, and at the RI time, respectively. This indicates that the vertical transport of cumulus convection has played a role to some extent. After the RI, the peak-value height of Q_2 continually falls (Fig. 2d), indicating that the cumulus convection is not so obvious. The peak-value height of Q_2 drops continually in the RW process (Figs. 2e-g), at 500, 600, and 700 hPa 24 h before RW, 12 h before RW, and at the RW time, respectively. It indicates that the cumulus convection is insignificant in the RW process of a TC.

4. The influence of diabatic heating on the TC rapid intensity change

4.1 Diagnostic equation

The complete vertical vorticity tendency equation has no omitted terms (Wu and Liu, 1999). In addition to the general advection, β-effect and divergence, the diabatic heating, friction and dissipation are accounted into the vertical vorticity tendency. The equation has been well applied in diagnosis of the formation and variation of the subtropical high, heavy rainfall cases, and explosive cyclone development (Wu et al., 1999; Liu et al., 1999; Zhou et al., 2004; Cui et al., 2002). In this paper, we attempt to use the equation to analyze the effects of diabatic heating on the TC rapid intensity change.

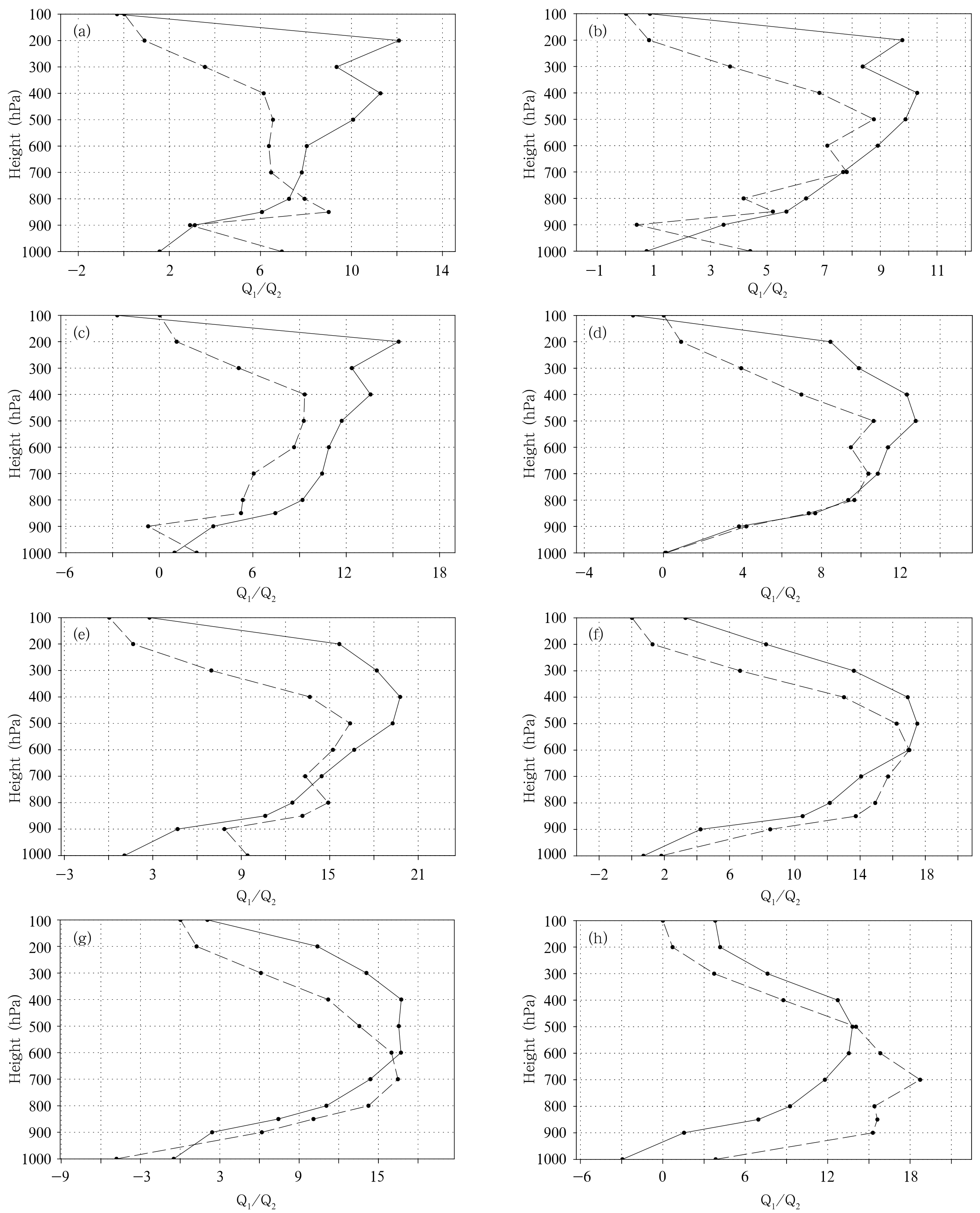

Fig. 2. Vertical profiles of areal averaged Q_1 and Q_2 (10^{-5} K s^{-1}) over a region within a radius of 5 latitude degrees to the composite TC center. (a)–(d) correspond to 24 and 12 h before the RI time, at the RI time, and 12 h after the RI time, respectively. (e)–(h) are the same as (a)–(d) but for the RW TC.

Under the assumption of no friction, no dissipation and slantwise vorticity effects, and by only keeping the external heating, the complete vertical vorticity equation is simplified into the following form ($\theta_z \neq 0$) (Wu and Liu, 1999; Liu et al., 1999):

$$\begin{aligned}\frac{\partial \varsigma}{\partial t} = &-(u\frac{\partial \varsigma}{\partial x}+v\frac{\partial \varsigma}{\partial y})-(u\frac{\partial f}{\partial x}+v\frac{\partial f}{\partial y})+(1-\kappa)\\ &\cdot(f+\varsigma)\frac{\omega}{p}-(f+\varsigma)\frac{Q}{\theta}+\frac{f+\varsigma}{\theta_z}\frac{\partial Q}{\partial z}\\ &-\frac{1}{\theta_z}\frac{\partial v}{\partial z}\frac{\partial Q}{\partial x}+\frac{1}{\theta_z}\frac{\partial u}{\partial z}\frac{\partial Q}{\partial y},\end{aligned} \quad (4)$$

where Q is the diabatic heating rate as in the thermodynamic equation, $\theta_z = \frac{\partial \theta}{\partial z}$, and other notations are conventional. Q can be replaced with the apparent heating source Q_1. The left hand side of Eq. (4) means vorticity tendency with a magnitude of 10^{-10} s^{-2}, and the terms on the right hand side denote, respectively, the vorticity advection (10^{-10}), β-effect (10^{-10}), upward motion (10^{-9}–10^{-10}), heating source (10^{-10}–10^{-11}), contribution of vertical non-uniform heating to the vorticity development (10^{-8}–10^{-9}), and contribution of horizontal non-uniform heating to the vorticity development (10^{-10}–10^{-11}).

According to the scale analysis, the vertical non-uniform heating $\frac{f+\varsigma}{\theta_z}\frac{\partial Q}{\partial z}$ is one to two orders larger in magnitude than the horizontal non-uniform heating $-\frac{1}{\theta_z}\frac{\partial v}{\partial z}\frac{\partial Q}{\partial x}$ and $\frac{1}{\theta_z}\frac{\partial u}{\partial z}\frac{\partial Q}{\partial y}$, and it is also one order or more larger than the upward motion and the heating source itself in the general heating occasions. In a real TC case, the magnitudes of Q, $(f+\varsigma)$, ω, and $\Delta\theta$ are 10^{-5} K s^{-1}, 10^{-4} s^{-1}, 10^{-3} hPa s^{-1}, and 10 K, respectively. Based on the above analysis, the vertical non-uniform heating makes the greatest contribution to the development of vorticity.

In the Northern Hemisphere, $f = 2\Omega\sin\varphi$ is always positive and increases with latitude. Generally, TCs are inertially stable ($f+\varsigma > 0$) and statically stable ($\theta_z = \frac{\partial \theta}{\partial z} > 0$).

4.2 Spatial non-uniform heating

4.2.1 Vertical non-uniform heating

$\left.\frac{\partial \varsigma}{\partial t}\right|_z^Q = \frac{f+\varsigma}{\theta_z}\frac{\partial Q}{\partial z}$ represents the contribution of vertical non-uniform heating to the vorticity development, and its effect on the rapid intensity change of the TC is discussed below. Overall, the maximum diabatic heating center is located near 200 hPa for the RI TC (Figs. 2a–c), but near 500 hPa for the RW TC (Figs. 2e–g).

Below the largest heating source and around the RI TC center, $\frac{\partial Q}{\partial z} > 0$ under 200 hPa results in $\left.\frac{\partial \varsigma}{\partial t}\right|_z^Q > 0$ and the genesis of positive vorticity, but $\frac{\partial Q}{\partial z} < 0$ above 200 hPa results in the genesis of negative vorticity. The vertical configuration is favorable to TC development, causing rapid intensification of the TC. The zero contour of $\left.\frac{\partial \varsigma}{\partial t}\right|_z^Q$ near the RI TC center reaches up to 200 hPa (Figs. 3a, 3b), and $\left.\frac{\partial \varsigma}{\partial t}\right|_z^Q$ increases while TC intensifies in the lower troposphere.

Near the RW TC center, $\frac{\partial Q}{\partial z} > 0$ exits below 500 hPa and $\frac{\partial Q}{\partial z} < 0$ above 500 hPa. Such a vertical pattern of the diabatic heating in the mid-upper troposphere produces negative vorticity and inhibits the TC development. The zero contour of $\left.\frac{\partial \varsigma}{\partial t}\right|_z^Q$ near the RW TC center is located near 500 hPa (Figs. 3c, 3d), and $\left.\frac{\partial \varsigma}{\partial t}\right|_z^Q$ decreases while the TC weakens in the lower troposphere.

In a word, near the TC center between 500 and 200 hPa, $\frac{\partial Q}{\partial z} > 0$ corresponds to RI of the TC, and $\frac{\partial Q}{\partial Z} < 0$ corresponds to RW of the TC. In the lower troposphere near the TC center, with the increasing of $\frac{f+\varsigma}{\theta_z}\frac{\partial Q}{\partial z}$, the value of vorticity increases. This favors RI of the TC, and vice versa.

4.2.2 Horizontal non-uniform heating

The contribution of horizontal non-uniform heating to vorticity development can be expressed as $\left.\frac{\partial \varsigma}{\partial t}\right|_x^Q = -\frac{1}{\theta_z}\frac{\partial v}{\partial z}\frac{\partial Q}{\partial x}$ and $\left.\frac{\partial \varsigma}{\partial t}\right|_y^Q = \frac{1}{\theta_z}\frac{\partial u}{\partial z}\frac{\partial Q}{\partial y}$. It is associated with the vertical wind shears $\frac{\partial u}{\partial z}$ and $\frac{\partial v}{\partial z}$. Using the thermal wind relationship $\frac{\partial u}{\partial z} = -\frac{g}{fT}\frac{\partial T}{\partial y}$ and $\frac{\partial v}{\partial z} = \frac{g}{fT}\frac{\partial T}{\partial x}$, the contribution of horizontal non-uniform heating turns into $\left.\frac{\partial \varsigma}{\partial t}\right|_x^Q = -\frac{g}{fT\theta_z}\frac{\partial T}{\partial x}\frac{\partial Q}{\partial x}$ and $\left.\frac{\partial \varsigma}{\partial t}\right|_y^Q = -\frac{g}{fT\theta_z}\frac{\partial T}{\partial y}\frac{\partial Q}{\partial y}$. These formulas indicate that

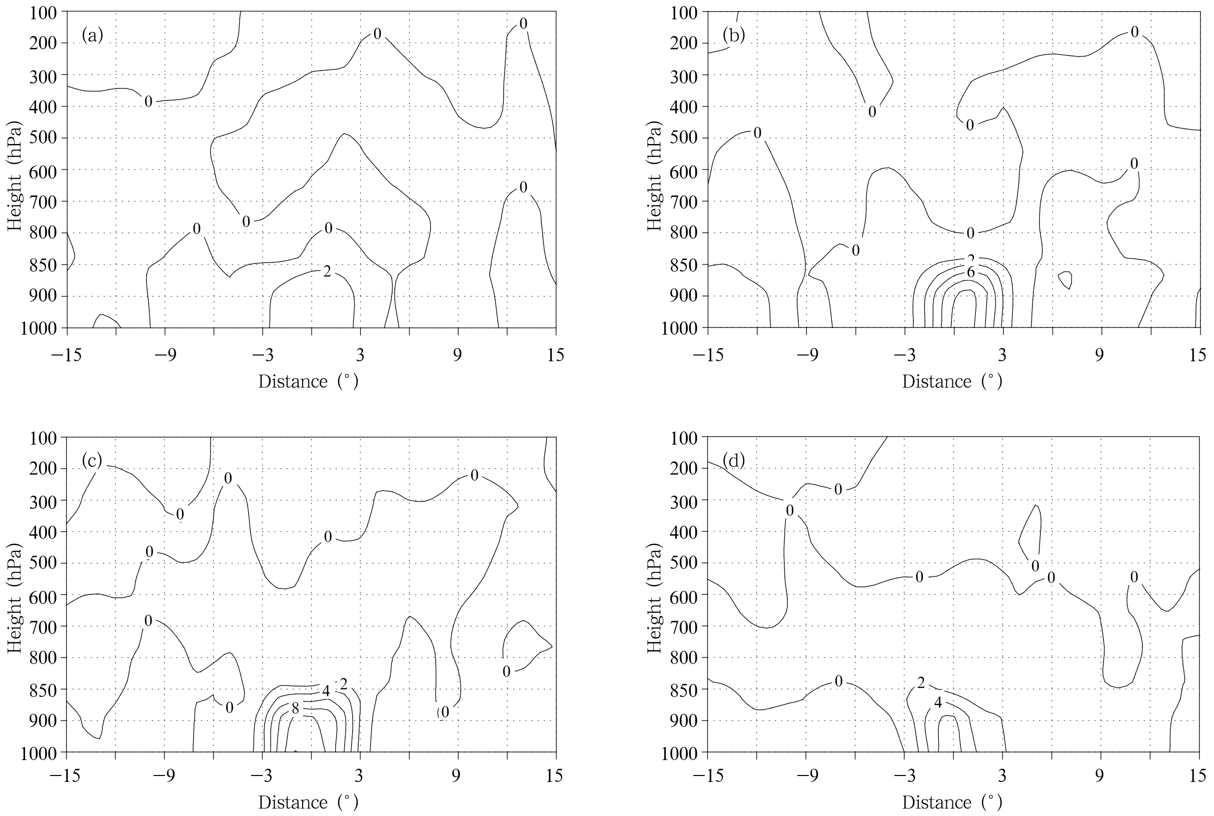

Fig. 3. Vertical cross-sections of the vertical non-uniform heating $\dfrac{f+\varsigma}{\theta_z}\dfrac{\partial Q}{\partial z}$ (10^{-9} s^{-2}) through the TC center (a) 24 h before the RI time, (b) at the RI time, (c) 24 h before the RW time, and (d) at the RW time.

when the horizontal non-uniform heating and the horizontal temperature change with the same phase, the anticyclonic vorticity grows, and on the contrary, the cyclonic vorticity grows, and this can be used to determine whether the TC would develop or not. In general, the contribution of horizontal non-uniform heating to RI of the TC is greater than that to RW of the TC (figure omitted).

In the complete vertical vorticity equation, the sum of the vertical heating and horizontal heating $\left(\dfrac{f+\varsigma}{\theta_z}\dfrac{\partial Q}{\partial z}-\dfrac{1}{\theta_z}\dfrac{\partial v}{\partial z}\dfrac{\partial Q}{\partial x}+\dfrac{1}{\theta_z}\dfrac{\partial u}{\partial z}\dfrac{\partial Q}{\partial y}\right)$ denotes the contribution of spatial non-uniform heating to the vorticity development. Near the TC center, the contribution of spatial non-uniform heating to the vorticity development of the RI TC is greater than that to the RW TC (Fig. 4). Similar to the evolution of the contribution of vertical non-uniform heating to the vorticity development, for the RI TC, the contribution of spatial non-uniform heating to the vorticity development becomes bigger and bigger, but it becomes smaller and smaller for the RW TC (figure omitted).

4.3 Upward motion and heating source

Upward motion $(1-\kappa)(f+\varsigma)\dfrac{\omega}{p}$ and heating source $-(f+\varsigma)\dfrac{Q}{\theta}$ are negative near the TC center throughout the troposphere (Fig. 5). Therefore, the effects of upward motion and heating source are different from that of the vertical non-uniform heating. They compensate the latent heat release in the vorticity evolution. The magnitudes of $\dfrac{f+\varsigma}{\theta_z}\dfrac{\partial Q}{\partial z}$, $(1-\kappa)(f+\varsigma)\dfrac{\omega}{p}$, and $-(f+\varsigma)\dfrac{Q}{\theta}$ are about 10^{-8}–10^{-9}, 10^{-9}–10^{-10}, and 10^{-10}–10^{-11} s^{-2}, respectively. Therefore, the effects of the upward motion and heating source are not enough to offset the effect of vertical non-uniform latent heat release.

4.4 Vorticity advection and β effect

The contribution of vorticity advection $-(u\dfrac{\partial\varsigma}{\partial x}+$

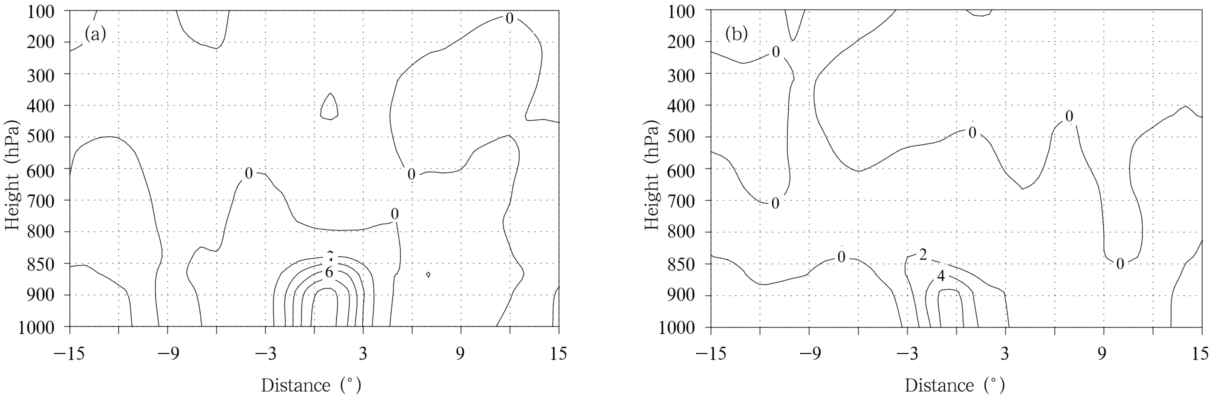

Fig. 4. Vertical cross-sections of the spatial non-uniform heating $\frac{f+\varsigma}{\theta_z}\frac{\partial Q}{\partial z}-\frac{1}{\theta_z}\frac{\partial v}{\partial z}\frac{\partial Q}{\partial x}+\frac{1}{\theta_z}\frac{\partial u}{\partial z}\frac{\partial Q}{\partial y}$ (10^{-9} s^{-2}) through the TC center at (a) the RI time and (b) the RW time.

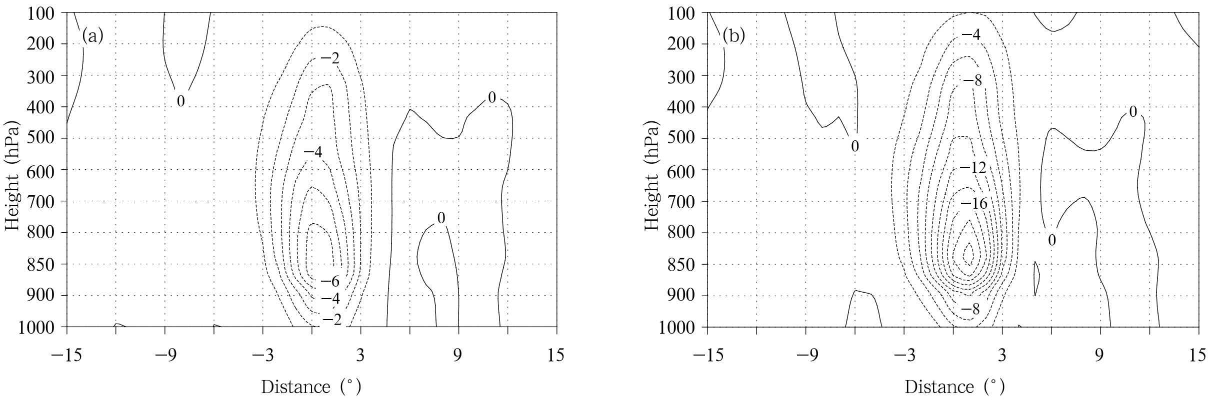

Fig. 5. Vertical cross-sections of (a) vertical motion $(1-\kappa)(f+\varsigma)\frac{\omega}{p}$ (10^{-9} s^{-2}) and (b) diabatic heating $-(f+\varsigma)\frac{Q}{\theta}$ (10^{-11} s^{-2}).

$v\frac{\partial \varsigma}{\partial y}$) and the β effect to the vorticity development for the RI TC are greater than those for the RW TC (figure omitted).

4.5 Local change of complete vertical vorticity

The cooperative effect of the terms at the right-hand side of the complete vorticity equation such as the vorticity advection, β-effect, vertical motion, heating source, and spatial non-uniform heating, is manifested in the complete vertical vorticity local change $\frac{\partial \varsigma}{\partial t}$.

$\frac{\partial \varsigma}{\partial t}$ increases near the TC center in the lower troposphere (Figs. 6a, 6b) for the RI TC, and vice versa (Figs. 6c, 6d). $\frac{\partial \varsigma}{\partial t}$ is obviously larger for the RI TC than that for the RW TC (Figs. 6b, 6d). Therefore, the growth of $\frac{\partial \varsigma}{\partial t}$ near the TC center is favorable to RI of the TC, and the decrease of $\frac{\partial \varsigma}{\partial t}$ leads to RW of the TC.

In summary, the different mechanisms for diabatic heating contributions to RI and RW of the TC are listed in Table 2.

5. Conclusions and discussion

Based on the NCEP FNL analysis data in 2000–2006, the thermodynamic mechanism for rapid intensity change of TCs over the coastal waters of China is investigated by using the composite analysis method. The main conclusions are given as follows:

(1) There exists the maximum apparent heating source Q_1 in the upper and lower troposphere near the RI TC center, and the lower-level Q_1 becomes larger while the TC intensifies. But for the RW TC, there exists the maximum Q_1 in the mid troposphere near

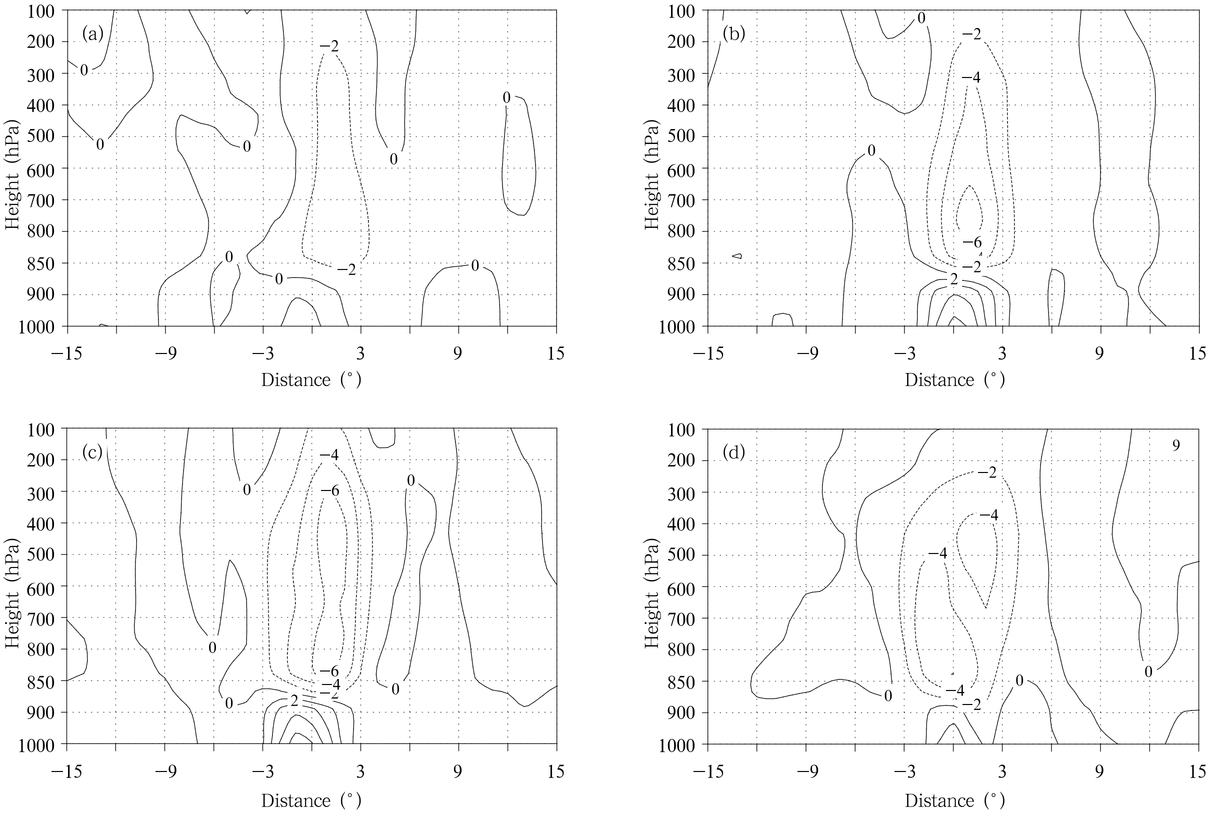

Fig. 6. Vertical cross-sections of the local tendency of vorticity $\frac{\partial \varsigma}{\partial t}$ (10^{-9} s^{-2}) through the TC center (a) 24 h before the RI time, (b) at the RI time, (c) 24 h before the RW time, and (d) at the RW time.

Table 2. A summary of the effect of diabatic heating on the rapid change of TC intensity

	RI TC	RW TC
Diabatic heating	Maximum apparent heating source Q_1 appears in the upper and lower troposphere near the TC center and the lower-level Q_1 increases as the TC intensifies	Maximum apparent heating source Q_1 appears in the mid troposphere near the TC center and Q_1 decreases as the TC weakens
	Diabatic heating shows an increasing trend	Diabatic heating shows a decreasing trend
	Peak-value height of the apparent moisture sink Q_2 continually rises	Peak-value height of the apparent moisture sink Q_2 continually falls
Vertical non-uniform heating	Maximum diabatic heating occurs in the upper troposphere near 200 hPa	Maximum diabatic heating occurs in the mid troposphere near 500 hPa
	$\frac{\partial Q}{\partial z} > 0$ between 500 and 200 hPa near the TC center	$\frac{\partial Q}{\partial z} < 0$ between 500 and 200 hPa near the TC center
	Vertical non-uniform heating $\frac{f+\varsigma}{\theta_z}\frac{\partial Q}{\partial z}$ tends to increase near the TC center in the lower troposphere	Vertical non-uniform heating $\frac{f+\varsigma}{\theta_z}\frac{\partial Q}{\partial z}$ tends to decrease near the TC center in the lower troposphere
Horizontal non-uniform heating	Horizontal non-uniform heating varies in phase with the horizontal temperature change	Horizontal non-uniform heating varies out of phase with the horizontal temperature change

the TC center, and Q_1 becomes smaller while the TC weakens. The maximum apparent moisture sink Q_2 is located in the mid troposphere. Q_2 becomes larger and its peak-value height rises while the TC intensifies, and vice versa. Strong cumulus convection is found in the mid-upper troposphere for the RI TC, but it is not obvious for the RW TC. During the TC rapid intensity change period, the peak-value height of Q_1 changes little, and it is roughly in the upper troposphere while the TC intensifies and in the mid troposphere while the TC weakens. The peak-value height of Q_2 rises continually while the TC intensifies, indicating that the vertical transport of cumulus convection has played a role to some extent. The peak-value height of Q_2 falls while the TC weakens, showing that the cumulus convection is not so obvious.

(2) The vertical non-uniform heating $\frac{f+\varsigma}{\theta_z}\frac{\partial Q}{\partial z}$ is the main contribution term to the vorticity development. When $\frac{\partial Q}{\partial z}$ is positive between 500 and 200 hPa near the TC center, the TC rapidly intensifies, and vice versa. This shows that the diabatic heating, which increases with latitude, corresponds to the RI TC, otherwise it corresponds to the RW TC. With the increasing of $\frac{f+\varsigma}{\theta_z}\frac{\partial Q}{\partial z}$, the vorticity value increases in the lower troposphere near the TC center, and this is favorable to the RI TC, and vice versa.

The above results may shed some lights on the prediction of the rapid intensity change of TCs over the coastal waters of China, especially on the prediction of the RI TC. In the real-time operational TC forecasting, the apparent heating source Q_1 can be calculated using observational data near the TC center in the mid-upper troposphere (500–200 hPa) as a practical prediction criterion. When it increases with height, the TC tends to intensify rapidly. Otherwise, the TC tends to rapidly weaken.

We also analyzed the thermodynamic characteristics of super Typhoon Saomai (2006) during its rapid intensity change period, and obtained similar conclusions to the above, which are not presented here. In general, the intensity change for a real TC may be related to several factors. For the specific mechanism of the TC rapid intensification, especially the thermodynamic one, we expect to conduct numerical experiments for a further analysis in the future.

REFERENCES

Anthes, R. A., 1982: Tropical cyclones: Their evolution, structure and effects. *Amer. Meteor. Soc.*, **19**(41), 11–64.

Cao Hongxing, 2005: Advances in atmospheric thermodynamics issues. *J. Appl. Meteor. Sci.*, **16**(4), 554–560. (in Chinese)

Chen Lianshou, Xu Xiangde, Luo Zhexian, et al., 2002: *Introduction to Tropical Cyclone Dynamics.* China Meteorological Press, Beijing, 185–210, 248–299.

Cui Xiaopeng, Wu Guoxiong, and Gao Shouting, 2002: Numerical simulation and isentropic analysis of frontal cyclones over the western Atlantic Ocean. *Acta Meteor. Sinica*, **60**(3), 385–399. (in Chinese)

Ding Yihui, 1989: *The Diagnostic and Analysis Method in Synoptic Dynamics.* Science Press, Beijing, 74–176, 145–149.

Emanuel, K. A., 1999: Thermodynamic control of hurricane intensity. *Nature*, **401**, 665–669.

Halverson, J. B., J. Simpson, G. Heymsfield, et al., 2006: Warm core of hurricane Erin diagnosed from high altitude dropsondes during CAMEX-4. *J. Atmos. Sci.*, **63**, 309–324.

Johnson, R. H., 1984: Partitioning tropical heat and moisture budgets into cumulus and mesoscale components: Implications for cumulus parameterization. *Mon. Wea. Rev.*, **112**, 1590–1601.

Liang Jianyin, Chen Zitong, Wan Qilin, et al., 2003: Diagnostic analysis of the landfall process tropical cyclone "Vongfong". *J. Tropical Meteorology*, **19**(Suppl.), 45–55. (in Chinese)

Liu Shida and Liu Shikuo, 1984: A model of bifurcation and catastrophe of the convection in atmosphere. *Acta Mechanica Sinica*, **16**(1), 10–18. (in Chinese)

Liu Shikuo and Ni Bingjian, 1983: The influence of inertial stability and stratification stability on typhoon development. Proceedings of the Conference on Typhoon (1983). Shanghai Science & Technology Press, Shanghai, 13–22.

Liu Yimin, Wu Guoxiong, Liu Hui, et al., 1999: The effect of spatially nonuniform heating on the formation and variation of subtropical high. Part III: Condensation heating and South Asian high and western Pacific subtropical highs. *Acta Meteor. Sinica*, **57**(5), 525–538. (in Chinese)

Schneider, R., and G. M. Barnes, 2005: Low-level kinematic, thermodynamic, and reflectivity fields associated with hurricane Bonnie (1998) at landfall. *Mon. Wea. Rev.*, **133**, 3243–3259.

Wu Guoxiong and Liu Huanzhu, 1999: Complete form of vertical vorticity tendency equation and slantwise vorticity development. *Acta Meteor. Sinica*, **57**(1), 1–15. (in Chinese)

——, Liu Yimin, and Liu Ping, 1999: The effect of spatially nonuniform heating on the formation and variation of subtropical high. Part I: Scale analysis. *Acta Meteor. Sinica*, **57**(3), 257–263. (in Chinese)

—— and Liu Yimin, 2000: Thermal adaptation, overshooting, dispersion, and subtropical anticyclone. Part I: Thermal adaptation and overshooting. *Chinese J. Atmos. Sci.*, **24**(4), 433–446. (in Chinese)

Wu Rongsheng, 2002: *Atmospherics Dynamics* (*Revised Edition*). Higher Education Press. Beijing, 310 pp.

Xia Youlong, Zheng Zuguang, and Liu Shida, 1995: The effects of heating in the inner core and the external part of typhoon on their intensity abrupt changes. *Acta Meteor. Sinica*, **53**(4), 424–430. (in Chinese)

Xu Xiangde, 1991: Study on influence factors of equilibria, destablization and catastrophe of nonlinear movement of axisymmetric vortex. *Chinese J. Atmos. Sci.*, **15**(2), 63–72. (in Chinese)

Xu Yamei, 2007: The numerical study of landfalling typhoon Bill (1988): Inner core structures and budgets of energy and moisture. *Acta Meteor. Sinica*, **65**(6), 877–887. (in Chinese)

Yan Jinghua, Ding Weiyu, Chen Zitong, et al., 2003: The modeling analyses on the kinetic and thermal features of tropical cyclone "Vongfong" (2002). *J. Tropical Meteorology*, **19**(Suppl.), 12–24. (in Chinese)

Yang Dasheng and Ding Minfang, 1985: The Nonlinear Mechanism of the Occurrence of Typhoons. Syposium on Typhoons in 1985. China Meteorological Press, Beijing, 231–243. (in Chinese)

Yanai, M., S. Esbensen, and J. H. Chu, 1973: Determination of bulk properties of tropical cloud clusters from large-scale heat and moisture budgets. *J. Atmos. Sci.*, **30**, 611–627.

Yu Yubin, Yang Changxian, and Yao Xiuping, 2007: The vertical structure characteristics analysis on abrupt intensity change of tropical cyclone over the offshore of China. *Chinese J. Atmos. Sci.*, **31**(5), 876–886. (in Chinese)

Zheng Zuguang and Xia Youlong, 1996: The intensity abrupt change in the inner core and external part of typhoon. *Acta Meteor. Sinica*, **54**(3), 294–302. (in Chinese)

Zhou Bing, He Jinhai, and Xu Haiming, 2004: Effect of torrential rain on variability of subtropical high. *J. Appl. Meteor. Sci.*, **15**(4), 394–406. (in Chinese)